Net Cloud Radiative Forcing at the Top of the Atmosphere in the Asian Monsoon Region

M. RAJEEVAN*

India Meteorological Department, Pune, India

J. SRINIVASAN

Centre for Atmospheric and Oceanic Sciences, Indian Institute of Science, Bangalore, India

(Manuscript received 16 October 1998, in final form 22 March 1999)

ABSTRACT

Based on the data from Earth Radiation Budget Experiment (ERBE), many investigators have concluded that the net cloud radiative forcing at the top of the atmosphere is small in the deep convective region of the Tropics. This conclusion has been shown to be invalid for the Asian monsoon region during the period June–September. The ERBE data have been used to show that in the Asian monsoon region the net cloud radiative forcing at the top of the atmosphere is negative and its magnitude exceeds 30 W m^{-2} in 25% of the grids in this region. The large negative net cloud radiative forcing in the Asian monsoon region during June–September has been shown to be on account of the presence of large amount of high clouds and the large optical depth of these clouds. This combination of high cloud amount and high optical depth occurs in the Asian monsoon region only. In the other deep convective regions of the Tropics, high clouds with large optical depths are present, but they do not cover a large area.

1. Introduction

The concept of cloud radiative forcing has been used extensively to study the impact of clouds on climate. Cloud radiative forcing at the top of the atmosphere is defined as the difference between the radiative fluxes with and without clouds. The observations from the Earth Radiation Budget Experiment (ERBE) provided the first accurate estimate of the modulation of longwave and shortwave radiative fluxes at the top of the atmosphere by clouds (Ramanathan et al. 1989). Using the ERBE data, Harrison et al. (1990) have examined the seasonal variation of cloud radiative forcing. A number of studies (Ramanathan et al. 1989; Harrison et al. 1990; Stephens and Greenwald 1991; Hartmann et al. 1992) have estimated that the global average shortwave cloud radiative forcing (SWCRF) and longwave cloud radiative forcing (LWCRF) are approximately -50 W m^{-2} and 30 W m^{-2}, respectively. The magnitude of the net cloud radiative forcing, which is defined as the sum of SWCRF and LWCRF, is generally larger in higher latitudes of the summer hemisphere. Hartmann and Doelling (1991) examined the net radiative effectiveness of clouds in terms of a cloud factor angle defined in coordinates of reflected solar radiation versus outgoing longwave radiation. Their study suggested that ratio of the solar to the longwave effect of cloud is about 1.85 based on the regression method and 1.55 based on the comparison of clear sky and total sky fluxes. Recently, Bony et al. (1997) examined the influence of sea surface temperature and large-scale circulation on cloud radiative forcing using National Centers for Environmental Prediction–National Center for Atmospheric Research (NCEP–NCAR) 40 yr reanalyses and ERBE datasets.

ERBE data have revealed that the deep clouds in the Tropics caused large changes in both longwave and shortwave radiative fluxes at the top of the atmosphere. The changes in the shortwave and longwave fluxes were of the same magnitude but opposite sign. Based on the ERBE data for the Indonesian region for April 1985, Kiehl and Ramanathan (1990) argued that there is a near cancellation between LWCRF and SWCRF at the top of the atmosphere in the deep convective regions of the region. They concluded therefore that the net cloud forcing is near zero in all tropical convective regions. Kiehl (1994) showed that the net cloud forcing in the equatorial Pacific is close to zero in April 1985. In many

* *Additional affiliation:* Jawaharlal Nehru Centre for Advanced Scientific Research, Bangalore, India.

Corresponding author address: Dr. J. Srinivasan, Centre for Atmospheric and Oceanic Sciences, Indian Institute of Science, Bangalore 560012, India.
E-mail: jayes@caos.iisc.ernet.in

papers published since, it has been assumed that this near cancellation of LWCRF and SWCRF is a fundamental feature of deep convective systems in the Tropics. Kiehl (1994) proposed an elegant theory to explain the near cancellation of the effects of LWCRF and SWCRF. He argued that the observed near cancellation in the Tropics is mainly a result of the tropical tropopause height being close to 16 km. He also suggested that the near cancellation is a ubiquitous feature in all tropical convective regions (either land or ocean). Pierrehumbert (1995) proposed a new theory for the regulation of the sea surface temperature in the Tropics based on the assumption that there is a near cancellation between LWCRF and SWRCF in the Tropics.

Recently, Pai and Rajeevan (1998) have examined the variations in net cloud forcing at the top of the atmosphere in the tropical Indian ocean region using ERBE data. They have demonstrated that the variations in cloud radiative forcing are strongly correlated with changes in high cloud amount but weakly correlated with changes in low or middle clouds. They have shown that the net cloud forcing at the top of the atmosphere can be large in July in the Indian Ocean when the amount of high clouds exceeds 50%. They argue that the net cloud radiative forcing in the warm pool of the west Pacific Ocean is not large because the amount of high clouds in this region does not exceed 50%. Most of the earlier studies on the net cloud forcing in the Tropics had focused their attention on the warm pool of the Pacific and not on the Indian Ocean or the Asian monsoon region. In the light of the results obtained by Pai and Rajeevan (1998), it is essential to reexamine the issue of near cancellation of the LWCRF and SWCRF in greater depth. This is necessary because the net cloud forcing at the top of the atmosphere has a direct impact on the dynamics and evolution of deep convective systems in the Tropics (also called the tropical convergence zones or TCZ). Neelin and Held (1987) have shown that the strength of the low-level convergence in the TCZ is directly proportional to the net radiation at the top of the atmosphere. If the net cloud forcing (at the top of the atmosphere) is near zero in the TCZ as claimed by Kiehl (1994), then one should expect that clouds should have lesser impact on dynamics and evolution of the TCZ. Sikka and Gadgil (1980) have argued, however, that cloud–radiation feedback may influence the meridional migration of TCZ. In this paper, we demonstrate that the net cloud radiative forcing is large in the Asian monsoon region during the period June–September and examine the factors that contribute to large net cloud radiative forcing in this region.

2. Data

We have used the ERBE and International Satellite Cloud Climatology Project (ISCCP) data for the period 1985–88 in our analysis. The ERBE S-4 data archive (Barkstrom 1984) consists of monthly mean all-sky and clear-sky radiative fluxes (longwave and shortwave) at the top of the atmosphere at 2.5° × 2.5° resolution. The ERBE data are derived from the radiance measurements by the *Earth Radiation Budget Experiment* and *NOAA-9* and *NOAA-10* satellites. Errors in individual clear and overcast scenes in ERBE data are estimated to be less than 2% and are much lower when time and space averages are performed (Harrison et al. 1990). The ISCCP provides cloud parameters such as cloud height, cloud optical thickness, and cloud amount from a global network of geostationary weather satellites and at least one polar orbiting satellite. We have used the cloud data from the ISCCP C-2 dataset (Rossow and Schiffer 1991). In ISCCP data, the clouds are classified into three types. They are high, middle, and low clouds. The high clouds (i.e., cloud tops above 440 hPa) are cirrus, cirrostratus–cirrocumulus, and deep convective clouds. The cloud parameters we have used are monthly mean values with the same spatial resolution as ERBE. Fu et al. (1990) and Weare (1993) provide evidence that ISCCP variables qualitatively reproduce important aspects of large-scale monthly averages. Comparisons of ISCCP high clouds with Stratospheric Aerosol and Gas Experiment (SAGE) II satellite measurements (Liao et al. 1995) and ground-based lidar observations (Minnis et al. 1993) indicate that there is good agreement between these data. In ISCCP data, high cloud optical depth or water content may include contributions from lower clouds.

The cloud radiative forcing is calculated as follows. The LWCRF is defined as

$$\text{LWCRF} = F_{\text{clr}} - F,$$

where F is the longwave radiative flux at the top of the atmosphere. The subscript clr indicates the value of F for a clear scene within the 2.5° × 2.5° box. LWCRF is usually positive.

The SWCRF is calculated as

$$\text{SWCRF} = S(\alpha_{\text{clr}} - \alpha),$$

where S is the monthly incoming solar flux at the top of the atmosphere and α is the total sky albedo of the earth–atmosphere system. Here α_{clr} is the clear-sky albedo of the earth atmosphere system. SWCRF is usually negative.

The net cloud radiative forcing is defined as the sum of SWCRF and LWCRF and whose sign depends upon the relative values of LWCRF and SWCRF.

We have considered the regions 30°S to 30°N and 30° to 180°E for the spatial analysis, and the region 0° to 30°N and 60° to 120°E for further detailed statistical analysis as shown in Fig. 1. The analysis has been performed for the months of January, April, and October, and the period June–September, which are summer monsoon months of the Northern Hemisphere.

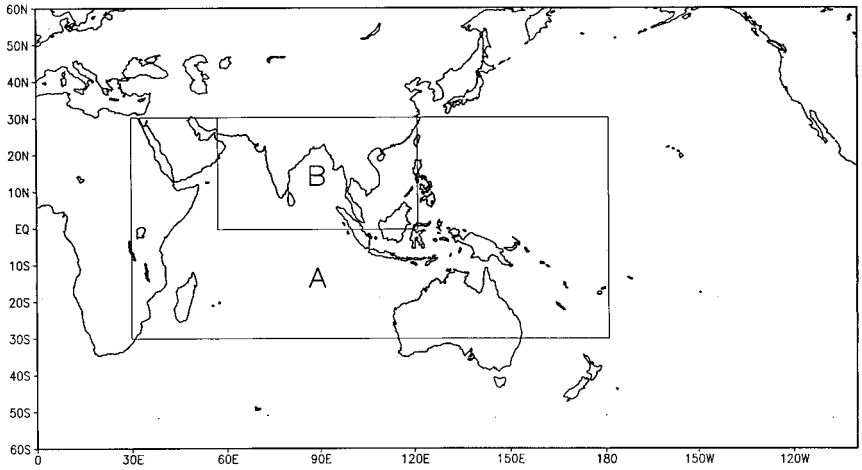

FIG. 1. Map highlighting the region of interest. The larger box, A (30°S–30°N, 30°–120°E), is used for spatial analysis whereas the smaller box, B (0°–30°N, 60°–120°E), is used for the detailed statistical analysis.

3. Cloud radiative forcing

a. Frequency distribution

The frequency distribution of net cloud radiative forcing (CRF) at the top of the atmosphere (TOA) in the Asian monsoon region (0°–30°N, 60°–120°E) for four representative months, January, April, July, and October, during the period 1985–88 are shown in Fig. 2. It can be seen that during January, April, and October, maximum frequency (about 45%) of net CRF is around

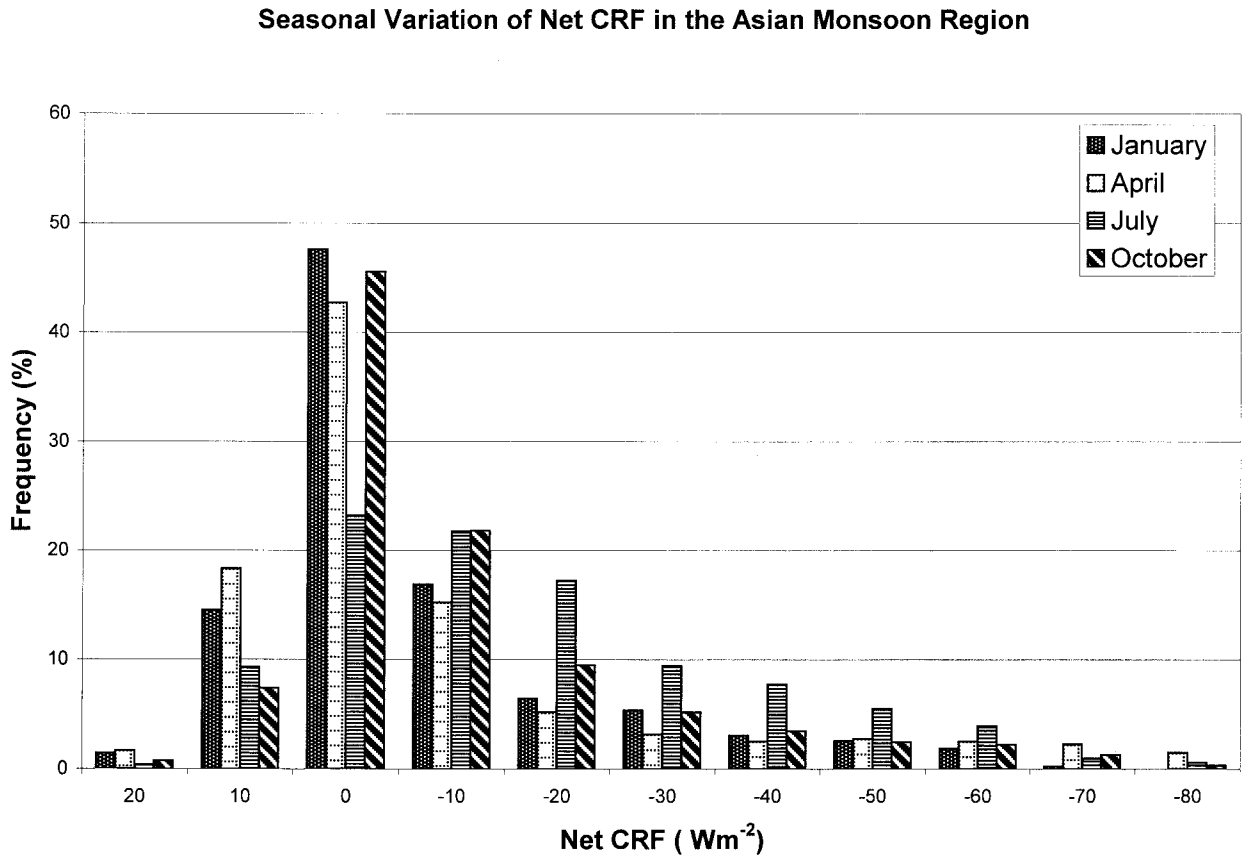

FIG. 2. Frequency distribution (in percentage) of ERBE net cloud radiative forcing for 10 W m^{-2} interval for Jan, Apr, Jul, and Oct. Period: 1985–88. Region: 0°–30°N, 60°–120°E.

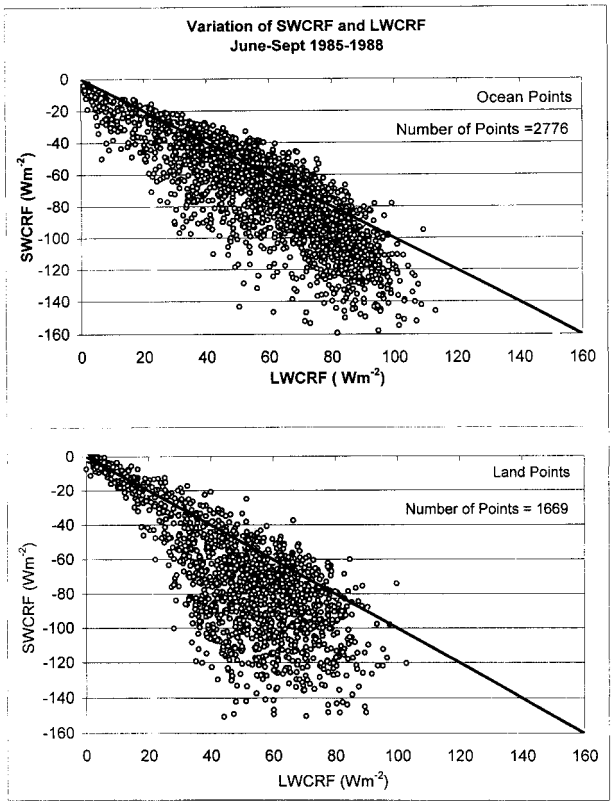

FIG. 3. Scatter relationship between longwave and shortwave cloud radiative forcing for land and oceanic regions. Period: Jun–Sep 1985–88. Total number of data points are 1669 and 2776, respectively, for land and ocean. Region: 0°–30°N, 60°–120°E.

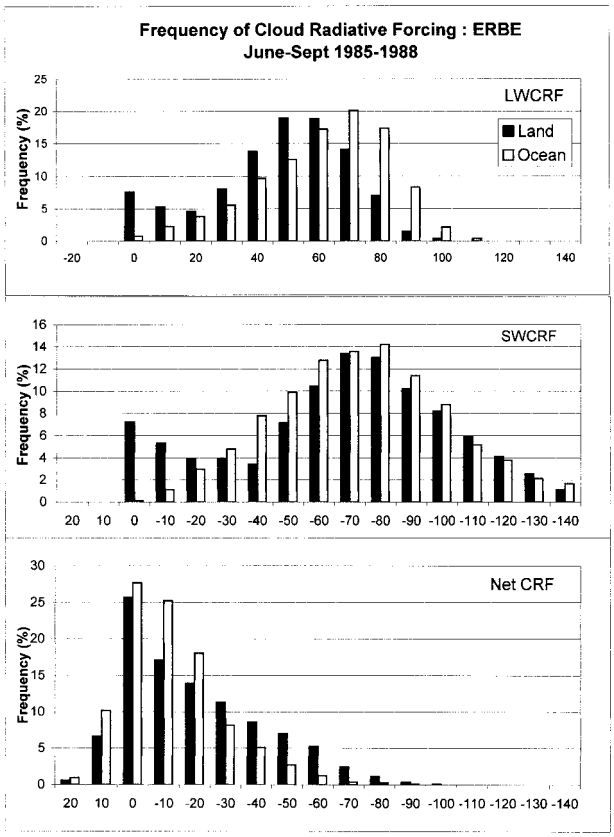

FIG. 4. Frequency distribution (in percentage) of ERBE longwave, shortwave, and net cloud radiative forcing for 10 W m^{-2} interval for land and oceanic regions. Period: Jun–Sep 1985–88. Total number of points: 1669 for land and 2776 for ocean. Region: 0°–30°N, 60°–120°E.

zero. Frequency of net CRF with magnitude exceeding 20 W m^{-2} is less than 25% during these months. However, during the month of July, appreciable differences are observed. The frequency of net CRF around zero (near cancellation between SWCRF and LWCRF) is only 22% (as opposed to about 45% during the other three months). There is also a long tail of large negative net CRF. The percentages of grid points with net CRF with magnitude exceeding 20 W m^{-2} for the months of January, April, July, and October are 19%, 20%, 45%, and 24%, respectively. The spatial analysis of net CRF (not shown) for the months of January, April, and October revealed that the net CRF of magnitude exceeding 20 W m^{-2} is mainly observed over the east coast of the Asian continent due to marine stratus clouds associated with midlatitude weather systems in which the longwave component of cloud radiative forcing is very small (Ramanathan et al. 1989). In this paper we focus our attention on the large negative net CRF that occurs during the monsoon months in the Asian region.

The scatter diagram relating LWCRF and SWCRF at the top of the atmosphere in the Asian monsoon region (0°–30°N, 60°–120°E) based on ERBE data is shown in Fig. 3 for ocean and land points separately. We have considered the period June–September during 1985–88. There were 4445 points in ERBE data (2776 points from ocean and 1669 points from land). Note that we have not filled the gaps in the ERBE clear-sky data by interpolation. The number of points in the ERBE data is less because the ERBE algorithm for identifying clear skies is unable to locate clear skies in the regions of persistent cloud cover. In the ERBE data, there is a near cancellation of SWCRF and LWCRF when LWCRF is below 80 W m^{-2} (40 W m^{-2}) over ocean (land). The SWCRF is larger than LWCRF when LWCRF is greater than 80 W m^{-2} (40 W m^{-2}) over ocean (land). Hence the near cancellation of SWCRF and LWCRF postulated by Kiehl (1994) will not occur in this region when LWCRF is above 80 W m^{-2} (40 W m^{-2}) over ocean (land).

The frequency distribution of cloud radiative forcing over the Asian monsoon region (0°–30°N, 60°–120°E) is shown in Fig. 4 for land and ocean regions separately. The peaks of LWCRF and SWCRF occur at a larger value over the oceanic regions when compared to land regions. The percentage of points with LWCRF more than 100 W m^{-2} is less than 2%, while the percentage of points with SWCRF lower than -100 W m^{-2} is more

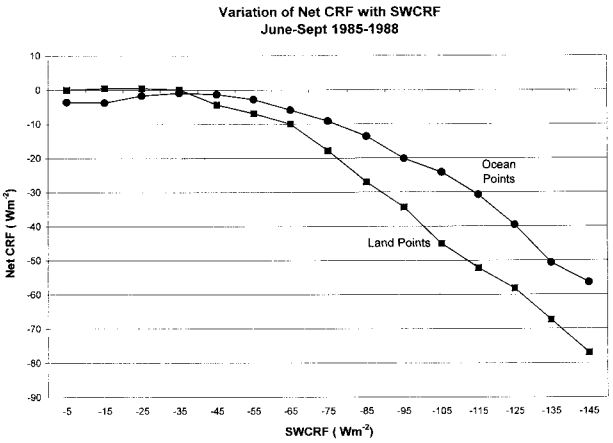

FIG. 5. Variation of net CRF with SWCRF bins of 10 W m^{-2} with respect to land and oceanic regions. Period: Jun–Sep 1985–88. Region: 0°–30°N, 60°–120°E.

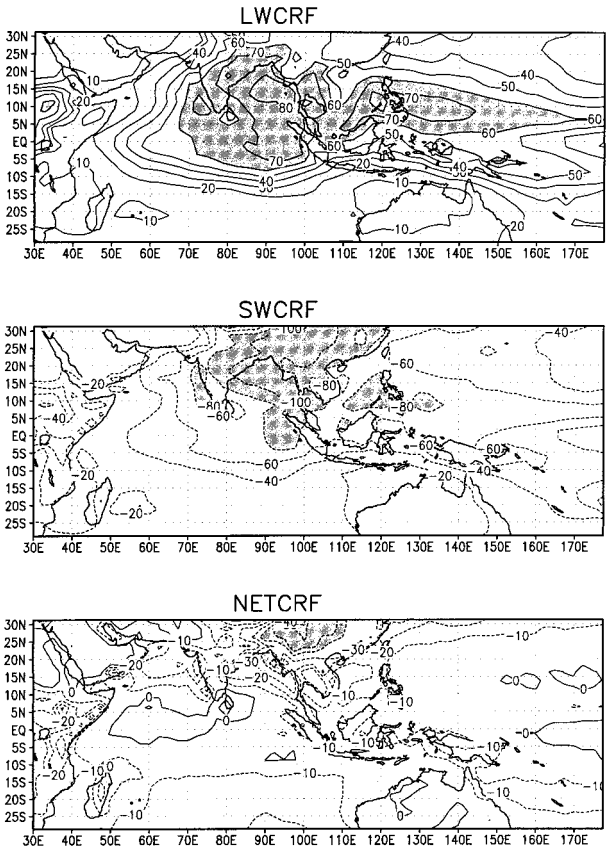

FIG. 6. Spatial variation of average LWCRF, SWCRF, and net CRF in W m^{-2}. Period: Jun–Sep 1985–88. LWCRF exceeding 60 W m^{-2}, SWCRF exceeding 80 W m^{-2}, and net CRF exceeding 40 W m^{-2} shaded.

than 20% over both land and ocean. This asymmetry in the frequency distribution of SWCRF and LWCRF leads to the asymmetry in the frequency distribution of net CRF. The frequency distribution of net CRF shows a maximum around zero (i.e., near–net cancellation between SWCRF and LWCRF) but there is a long tail indicating the existence of regions with large negative cloud forcing both over land and ocean. The percentage of points with magnitude of negative net CRF exceeding 30 W m^{-2} is around 36% over land and 18% over ocean. Note that the spatial extent of oceanic and land regions considered for the data analysis is not the same. The variation of net cloud forcing with SWCRF (in 10 W m^{-2} bins) is shown in Fig. 5. The net cloud forcing is close to zero at small SWCRF but increases rapidly once the magnitude of negative SWCRF exceeds 45 W m^{-2}. Over the regions with larger shortwave cloud radiative forcing, the magnitude of net CRF is more over land than over ocean.

b. Spatial patterns

The spatial patterns of LWCRF, SWCRF, and net CRF for the period June–September 1985–88, calculated using the ERBE data, is shown in Fig. 6. Larger LWCRF is observed over the southern Bay of Bengal and the equatorial east Indian Ocean. The negative net cloud forcing with its magnitude exceeding 30 W m^{-2} is observed over the northern Bay of Bengal and adjoining land areas over east Asia. These values are the averages over 16 months and hence are smaller than the values of some of the months. For example, if the values of net cloud forcing for July (1985–88) is computed, the values of net cloud forcing in the northern Bay of Bengal are as high as -50 W m^{-2}. Thus we find that even though there is a near cancellation between shortwave and longwave cloud forcing in many areas of the Tropics, large net negative cloud forcing is observed over the Asian monsoon region. The value of net cloud forcing is higher than the uncertainty limit of ERBE data (± 10 W m^{-2})

4. Relationships with cloud properties

The spatial distribution of average high cloud amount and optical depth over the Asian monsoon region is shown in Fig. 7. The optical depth of high clouds is computed as a weighted average of the optical depth of cirrus, cirrostratus, and deep convective clouds. High cloud amount exceeds 50% over the Bay of Bengal and adjoining land areas of the Asian monsoon region. It may be mentioned that over the west Pacific, where Kiehl and Ramanathan (1990) examined the net radiative forcing, the high cloud amounts do not exceed 50%. Similarly high optical depth exceeding 14 was observed over the northern Bay of Bengal and the Asian monsoon region. Over the west Pacific, clouds with large optical depth are, however, not observed. The spatial pattern of high cloud amount and optical depth are similar to the spatial pattern of net CRF (Fig. 6). The magnitude of net cloud forcing exceeds 30 W m^{-2} in the Asian monsoon region and occurs in regions with optical depth of

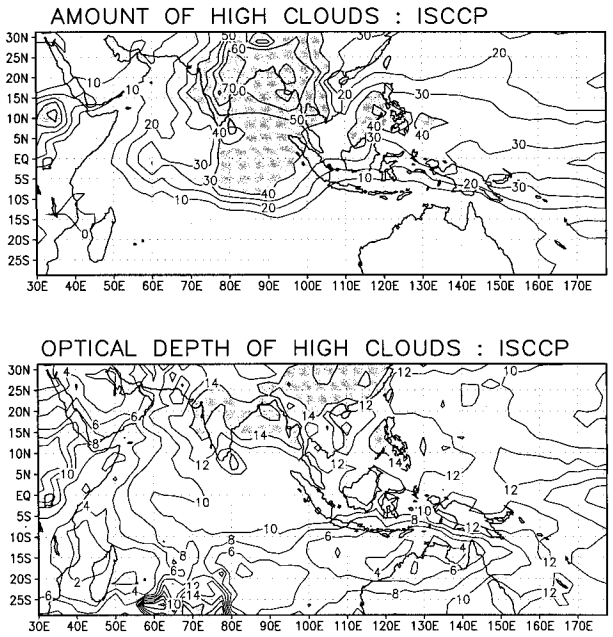

FIG. 7. (a) Spatial distribution of frequency of high clouds (%) and (b) optical depth of high clouds derived from ISCCP data. Period: Jun–Sep 1985–88. Amounts exceeding 40% and optical depth exceeding 14 shaded.

high clouds more than 14. Thus large negative net forcing occurs in regions with large amounts of optically thick high clouds. This aspect is further examined by averaging SWCRF and LWCRF with equal bins of high cloud optical depth. The data have been divided into six equal bins as shown in Fig. 8. The LWCRF reaches an asymptotic value around 60 W m^{-2} when optical depth of high clouds exceeds 10. The SWCRF increases rapidly when the optical depth increases from 10 to 14 but reaches an asymptote of -100 W m^{-2} when the optical depth exceeds 14. The rate of change of SWCRF with high cloud optical depth is much larger than that of LWCRF once the mean optical depth goes above 10. Similarly, the variation of SWCRF and LWCRF as a function high cloud amount is shown in Fig. 9. It can be seen that both SWCRF and LWCRF increase with increases in high cloud amount. When the high cloud amount is larger than 50%, the rate of increase of SWCRF with high cloud amount becomes more than that of LWCRF. This difference is, however, not as prominent in case of the variation of SWCRF and LWCRF with high cloud optical depth (Fig. 8). The observed large negative net forcing over the Asian monsoon region is associated with a large amount of high clouds with large optical thickness. In this respect, the Asian monsoon region is unique and similar conditions are not observed in the other deep convective regions of the Tropics (i.e., Pacific Ocean, Africa, or Amazon region). This is demonstrated in Fig. 10. The percentage of high clouds and the percentage of the region with high cloud optical depth above 12 is shown for different

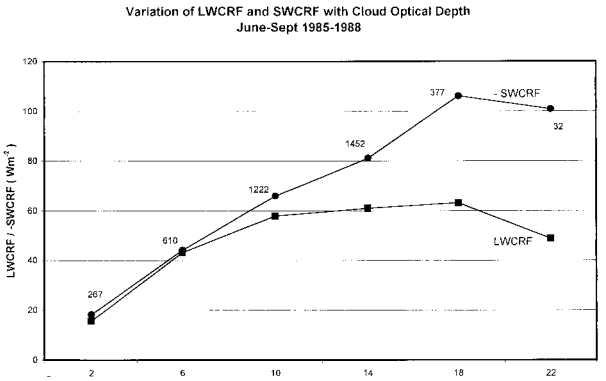

FIG. 8. Variation of longwave and negative shortwave cloud radiative forcing with high cloud optical depth bins of 4. Period: Jun–Sep 1985–88. Region: 0°–30°N, 60°–120°E. The numbers near the data points in the diagram indicate the total number of data points in the respective bins.

deep convective regions of the Tropics in 1988. Note that the regions have been chosen such that their spatial extent (20° lat × 20° long) is same for all regions. We find that in July and August the Asian monsoon region shows the unique combination of large amount of high clouds with large optical depth. In the Amazon region the optical depth of high clouds is almost as large as the Asian monsoon region, but the percentage of high cloud amount is much smaller. Thus the combination of large amount of high clouds and high clouds with large optical depth is seen in the Asian monsoon region only.

5. Conclusions

We have shown that the net cloud radiative forcing over the Asian monsoon region is large and negative by using the ERBE data for the period June–September during 1985–88. We have also shown that the large negative net cloud forcing over the Asian monsoon re-

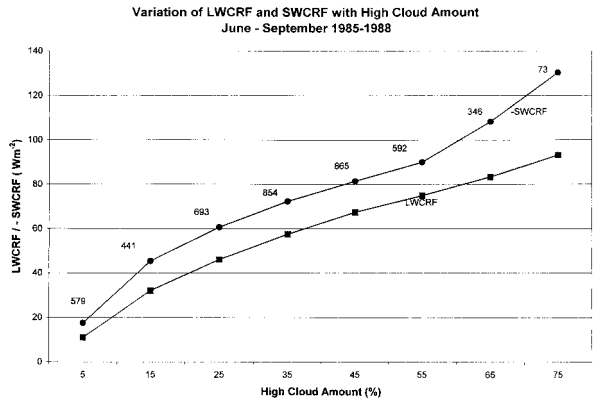

FIG. 9. Variation of longwave and negative shortwave cloud radiative forcing with high cloud amount bins of 10. Period: Jun–Sep 1985–88. Region: 0°–30°N, 60°–120°E. The numbers near the data points in the diagram indicate the total number of data points in the respective bins.

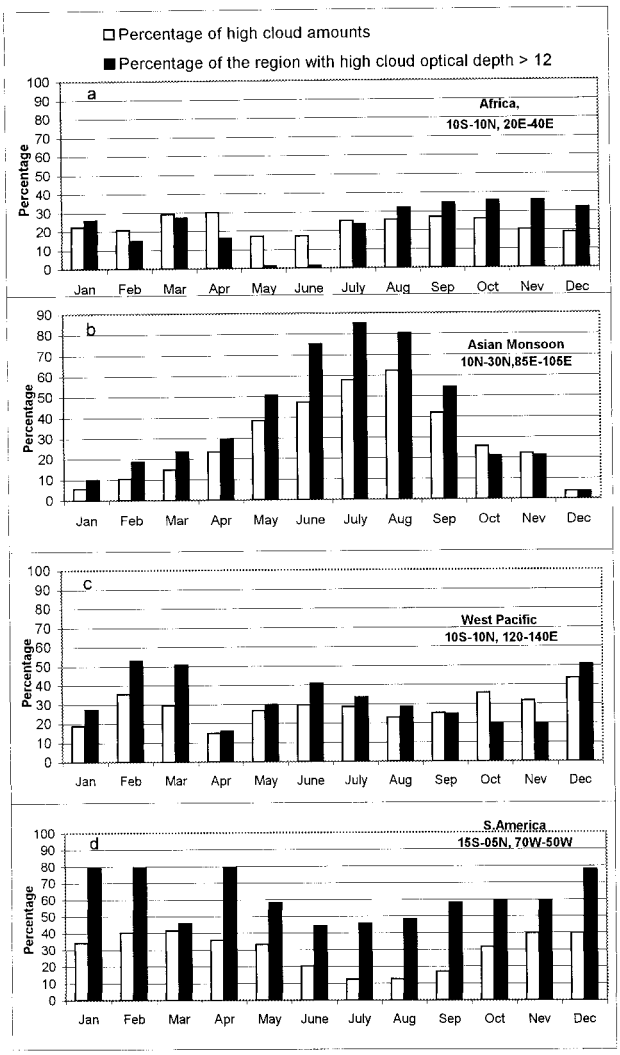

FIG. 10. Monthly variation of the percentage of the region with high cloud amount more than 50% and high cloud optical depth more than 12 in the year 1988 in four convective region of the Tropics. (a) Africa, (b) Asian monsoon region, (c) west Pacific, and (d) South America. Data source: ISCCP.

gion is due to presence of optically thick (optical thickness exceeding 14) high clouds (amounts exceeding 50%). At large optical depths, the effect of cloud albedo exceeds the cloud greenhouse effect and hence these clouds cause large negative net cloud forcing. In the equatorial Pacific, the high clouds with large optical thickness are not predominant. Hence, the previous studies that focused their attention primarily on the equatorial Pacific concluded that the net cloud forcing in the deep convection region of the Tropics is close to zero. Neelin and Held (1987) have shown that the net radiation at the TOA represents the total energy convergence in the continental TCZ. If the net cloud radiative forcing is negative in a continental region, then the cloud-radiation feedback in the TCZ is negative. Based on the results reported in this paper, we conclude that the cloud–radiation feedback is negative in the deep convective regions of Asia during June–September. We must mention, however, that the clear-sky data are not available in ERBE for some grids in the Asian monsoon region during the months of July and August. This is on account of the existence of persistent high cloud cover. Hence the estimate of the magnitude of the net cloud radiative forcing obtained here may be somewhat lower than the actual value. Moreover, the clear-sky identification algorithm used in ERBE has problems in identifying clear pixels within deep convective regions (Hartmann and Doelling 1991). The algorithm introduces a bias because it labels clear-sky regions with high humidity (in deep convective region in the Tropics) as cloudy regions. This bias may have an impact on our results.

Many atmospheric general circulation models do not simulate the mean structure of the Asian monsoon correctly. This could be due to their inability to simulate correctly the cloud radiative properties in the Asian monsoon region. Bony et al. (1997) and Weare (1997b) have shown that some GCMs do not simulate correctly the cloud radiative properties. Weare (1997a) has shown that longwave cloud forcing is strongly related to high cloud amounts and shortwave cloud forcing is better related to high cloud amounts and high cloud optical depth. While low clouds make little contribution to LWCRF, they make a substantial contribution to SWRCF. In highly convective regions in the Tropics the albedo and outgoing longwave radiation are significantly affected by variations in cloud structure as well as cloud amount (Hartmann and Doelling 1991). These variations cause an asymmetry in the distribution as shown in the frequency diagrams (Fig. 4). Poetzsch Heffter et al. (1995) examined nine types of ISCCP clouds and their effect on cloud radiative forcing. They have suggested that the cloud type 9 (cirrostratus and cumulonombus, with mean optical depth >10, cloud albedo $>\sim 0.6$, and IR transmission $<0.4\%$) makes the largest single contribution to the net cloud forcing. This is consistent with the results obtained in this study. Recently, Heymsfield et al. (1998) have measured the cloud forcing in highly reflective optically thick cirrus clouds over the equatorial Pacific using in situ and remote sensing data on a $0.25^\circ \times 0.25^\circ$ grid. They have shown that in these clouds albedo is greater than 0.40 and the SWCRF is much higher than the LWCRF. They obtain a much larger net cloud forcing in the equatorial Pacific than that reported in the previous studies because they used a much finer grid in their analysis compared to the conventional $2.5^\circ \times 2.5^\circ$ grid. A similar observational study of the cloud radiative properties over Asian monsoon region will be necessary to document the unique features of the deep convective clouds in this region.

Acknowledgments. The work was carried out when the first author (MR) was at the Centre for Atmospheric and Oceanic Sciences, Indian Institute of Science, Ban-

galore, under the Visiting Fellowship Programme of Jawaharlal Nehru Centre for Advanced Scientific Research (JNCASR), Bangalore. The first author is grateful to JNCASR for offering the visiting fellowship for this collaborative work and to the DGM of IMD for granting permission to avail this fellowship and for his encouragement, and to Dr. U. S. De, ADGM(R), for his encouragement and help. We are also thankful to Prof. Sulochana Gadgil for her encouragement and valuable suggestions, and to Mr. Arvind Gambheer and Ms. Suman for their help in computation. The ERBE and ISCCP datasets were obtained from NASA Langley Research Center, Distributed Active Archive Centre (DAAC), for which we are grateful to NASA. The second author (JS) would like to thank Indian Space Research Organization for financial support to carry out this project. We thank the referees for several useful suggestions.

REFERENCES

Barkstrom, B. R., 1984: The Earth Radiation Budget Experiment (ERBE). *Bull. Amer. Meteor. Soc.,* **65,** 1170–1185.

Bony, S., K. M. Lau, and Y. C. Sud, 1997: Sea surface temperature and large-scale circulation influences on tropical greenhouse effect and cloud radiative forcing. *J. Climate,* **10,** 2055–2077.

Fu, R., A. Del Genio, and W. B. Rossow, 1990: Behavior of the convective clouds in the tropical Pacific deduced from ISCCP radiances. *J. Climate,* **3,** 1129–1152.

Harrison, E. F., B. R. Barkstrom, V. Ramanathan, R. D. Cess, and G. G. Gibson, 1990: Seasonal variation of cloud radiative forcing derived from the Earth Radiation Budget Experiment. *J. Geophys. Res.,* **95,** 18 687–18 703.

Hartmann, D. L., and D. Doelling, 1991: On the net radiative effectiveness of clouds. *J. Geophys. Res.,* **96,** 869–891.

——, M. E. Ockert-Bell, and M. L. Michelson, 1992: The effect of cloud type on earth's energy balance: Global analysis. *J. Climate,* **5,** 1281–1304.

Heymsfield, A. J., G. M. McFarquhar, W. D. Collins, J. A. Goldstein, F. P. J. Valero, J. Spinhirne, W. Hart, and P. Pilewskie, 1998: Cloud properties leading to highly reflective tropical cirrus: Interpretations from CEPEX, TOGA COARE, and Kwajalein, Marshall Islands. *J. Geophys. Res.,* **103** (D8), 8805–8812.

Kiehl, J. T., 1994: On the observed near cancellation between longwave and shortwave cloud forcing in tropical regions. *J. Climate,* **7,** 559–565.

——, and V. Ramanathan, 1990: Comparison of cloud forcing derived from the Earth Radiation Budget Experiment with that simulated by the NCAR community climate model. *J. Geophys. Res.,* **95,** 11 679–11 698.

Liao, Y., W. B. Rossow, and D. Rind, 1995: Comparisons between SAGE II and ISCCP high-level clouds. Part 1. Global and zonal mean cloud amounts. *J. Geophys. Res.,* **100,** 1121–1135.

Minnis, P., P. W. Heck, and D. F. Young, 1993: Inference of cirrus cloud properties using satellite-observed visible and infrared radiance. Part II: Verification of theoretical cirrus radiative properties. *J. Atmos. Sci.,* **50,** 1305–1322.

Neelin, J. D., and I. M. Held, 1987: Modeling tropical convergence zone based on moist static energy budget. *Mon. Wea. Rev.,* **115,** 3–12.

Pai, D. S., and M. Rajeevan, 1998: Clouds and cloud radiative forcing over tropical Indian ocean and their relationship with sea surface temperature. *Curr. Sci.,* **75,** 372–381.

Pierrehumbert, R. T., 1995: Thermostats, radiator fins, and the local runaway greenhouse. *J. Atmos. Sci.,* **52,** 1784–1806.

Poetzsch Heffter, C., Q. Liu, E. Ruprecht, and C. Simmer, 1995: Effect of cloud types on the Earth Radiation Budget calculated with the ISCCP C1 dataset: Methodology and initial results. *J. Climate,* **8,** 829–843.

Ramanathan, V., R. D. Cess, E. F. Harrison, P. Minnis, B. R. Barkstrom, E. Ahmad, and D. Hartmann, 1989: Cloud-radiative forcing and climate: Results from the Earth Radiation Budget Experiment. *Science,* **243,** 57–63.

Rossow, W. B., and R. A. Schiffer, 1991: ISCCP cloud data products. *Bull. Amer. Meteor. Soc.,* **72,** 2–20.

Sikka, D. R., and S. Gadgil, 1980: On the maximum cloud zone and the ITCZ over Indian longitude during the southwest monsoon. *Mon. Wea. Rev.,* **108,** 1840–1853.

Stephens, G. L., and T. J. Greenweld, 1991: The Earth's radiation budget and its relation to atmospheric hydrology. Part 2. Observations of cloud effects. *J. Geophys. Res.,* **96,** 15 325–15 340.

Weare, B. C., 1993: Multi-year statistics of selected variables from the ISCCP data set. *Quart. J. Roy. Meteor. Soc.,* **119,** 795–808.

——, 1997a: Climatic variability of cloud radiative forcing. *Quart. J. Roy. Meteor. Soc.,* **123,** 1055–1073.

——, 1997b: Comparison of NCEP–NCAR cloud radiative forcing reanalyes with observations. *J. Climate,* **10,** 2200–2209.